



ACOUSTIC WAVE SCATTERING FROM IMMERSED TRANSVERSELY ISOTROPIC CYLINDERS COVERED BY ISOTROPIC CLADDING

Sina Sodagar^{*1}, Farhang Honarvar¹, and Anthony N. Sinclair²

¹Faculty of Mechanical Engineering,
K. N. Toosi University of Technology, P.O. Box 16765-3381, Tehran, Iran

²Department of Mechanical and Industrial Engineering, University of Toronto,
5 King's College Road, Toronto, Ontario M5S 3G8, Canada
ssodagar@alborz.kntu.ac.ir

Abstract

An analytical model is developed for the scattering of acoustic waves from an immersed transversely isotropic rod covered by a cylindrical isotropic cladding. The mathematical formulation is derived for the far-field backscattered amplitude spectrum resulting from oblique insonification of the clad rod. It has been observed that when interacting with mechanical waves, transversely isotropic materials show two different behaviors. Consequently, they can be classified in two groups as type I and type II. In this paper, the frequency spectra and phase diagrams of these two types of transversely isotropic cylinders are studied. It is shown that in type I, similar to isotropic materials, at incidence angles larger than the second critical angle, no elastic wave can penetrate into the cylinder and the incident wave is completely reflected. Therefore, beyond the second critical angle, there is no resonance frequency in the frequency spectrum and phase diagram. However, in type II transversely isotropic materials, even beyond the second and third critical angles, resonance frequencies can be observed.

INTRODUCTION

Acoustic wave scattering from multi-layered cylindrical components has been considered in various applications such as the detection of underwater targets or nondestructive evaluation (NDE) of multi-layered components.

Flax and Neubauer [1] developed a mathematical model for predicting the scattered pressure field of a two-layered absorptive cylindrical shell with different fluid media inside and outside. Gaunaurd [2] studied the acoustic wave scattering from a hollow elastic cylinder covered by a viscoelastic coating. The oscillations in the cylinder cross-section due to the resonances in the shell and coating materials

were calculated and plotted for the low frequency range. Sinai [3] computed the scattered pressure field from a fluid-loaded two-layered cylinder for a range of frequencies, material parameters, and emitter and detector functions.

These studies are mostly concerned with isotropic cylinders and shells. In the NDE of cylindrical components, such as wires, rods, and pipes, the sample is usually transversely isotropic due to the processes used in manufacturing of these products. Transverse isotropy provides higher strength to stiffness ratio along the cylinder axis and hence, it is usually desirable. In 1996, Honarvar and Sinclair [4] used a normal-mode expansion based on decomposition of displacement field to calculate the scattered pressure field of an immersed transversely isotropic cylinder. They also formulated the problem of scattering of an obliquely incident plane acoustic wave from an infinite solid elastic clad rod [5].

In 2000, Ahmad and Rahman classified transversely isotropic materials into two groups as type I and type II [6]. They showed that an extra critical angle is observed in scattering of waves from type II materials. Honarvar and Sinclair showed that in type I materials, the normal stiffness along the cylinder axis is stronger than the normal stiffness in the isotropic plane and in type II materials it is the reverse [7]. In 2005, the authors developed a mathematical model for the scattering of acoustic waves from an immersed clad rod with transversely isotropic core [8]. In this paper, scattering of acoustic waves from a clad rod with transversely isotropic core will be considered. Using the calculated frequency spectra and phase diagrams, the behavior of type I and type II transversely isotropic cylinders are studied.

MATHEMATICAL FORMULATION

In the mathematical model, an infinite plane acoustic wave of frequency $\omega/2\pi$ incident at an angle α on a submerged isotropic clad-transversely isotropic rod of infinite length is considered, see Fig. 1. A cylindrical coordinate system (r, θ, z) is chosen with the z direction coincident with the axis of the cylinder. The pressure p_i of the incident plane wave external to the cylinder at a point $M(r, \theta, z)$ is represented by [9],

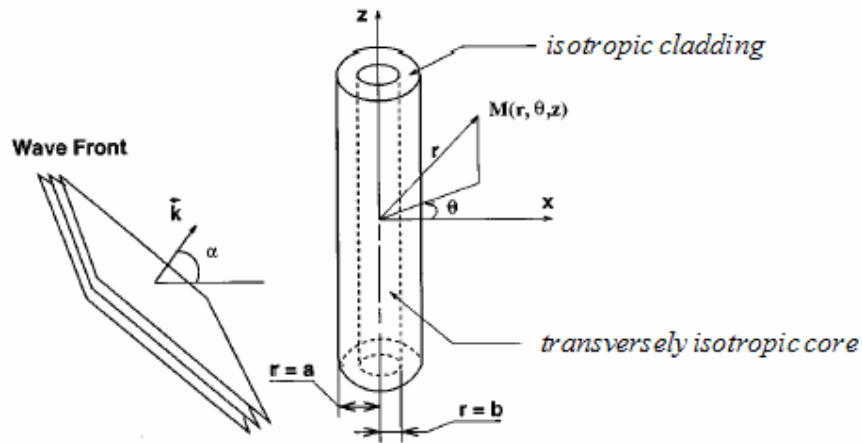


Fig. 1- Geometry of a plane wave obliquely incident on a submerged clad rod.

$$p_i = p_0 \sum_{n=0}^{\infty} \varepsilon_n i^n J_n(k_{\perp} r) \cos(n\theta) e^{i(k_z z - \omega t)} \quad (1)$$

where $k_z = k \sin \alpha$, $k_{\perp} = k \cos \alpha$ and $k = \omega / c$, c is the compression wave velocity in the liquid medium outside the cylinder, ε_n is the Neumann factor ($\varepsilon_n = 1$ for $n = 0$, and $\varepsilon_n = 2$ for $n > 0$), p_0 is the incident pressure wave amplitude, and J_n is the Bessel function of the first kind of order n . The outgoing scattered wave pressure p_s , at point M must be symmetrical about $\theta = 0$ and, therefore of the form,

$$p_s = p_0 \sum_{n=0}^{\infty} \varepsilon_n i^n A_n H_n^{(1)}(k_{\perp} r) \cos(n\theta) e^{i(k_z z - \omega t)} \quad (2)$$

where $H_n^{(1)}$ is the Hankel function of the first kind of order n , and A_n are the unknown scattering coefficients. The cylinder is composed of two parts: a transversely isotropic rod and isotropic cladding. In each part, the corresponding formulations are derived and necessary boundary conditions are applied to determine unknown coefficients.

Transversely Isotropic Rod

In a transversely isotropic rod, the displacement vector can be written in terms of three scalar potential functions ϕ , χ and ψ [10],

$$u = \nabla \phi + \nabla \times (\chi \hat{e}_z) + a \nabla \times \nabla \times (\psi \hat{e}_z), \quad (3)$$

where a is the radius of the rod. By substituting Eq. (3) in equations of motion and using general Hook's law, a set of three equations of motion in terms of ϕ , ψ , and χ is obtained [4]. To solve this set of equations, the normal mode expansion technique is used. Solutions should have the following forms:

$$\begin{aligned} \phi &= \sum_{n=0}^{\infty} B_n J_n(sr) \cos n\theta e^{i(k_z z - \omega t)} \\ \psi &= \sum_{n=0}^{\infty} C_n J_n(sr) \cos n\theta e^{i(k_z z - \omega t)} \\ \chi &= \sum_{n=0}^{\infty} D_n J_n(sr) \sin n\theta e^{i(k_z z - \omega t)} \end{aligned} \quad (4)$$

Substituting Eq. (4) in Eq. (3) and applying it to the equations of motion indicates that the potential functions should be of the form:

$$\begin{aligned}
 \phi &= \sum_{n=0}^{\infty} [B_n J_n(s_1 r) + q_2 C_n J_n(s_2 r)] \cos n\theta e^{i(k_z z - \omega t)} \\
 \psi &= \sum_{n=0}^{\infty} [q_1 B_n J_n(s_1 r) + C_n J_n(s_2 r)] \cos n\theta e^{i(k_z z - \omega t)} \\
 \chi &= \sum_{n=0}^{\infty} D_n J_n(s_3 r) \sin n\theta e^{i(k_z z - \omega t)}
 \end{aligned} \tag{5}$$

where the parameters q_1 , q_2 , s_1 , s_2 and s_3 are defined in Ref. [4].

Isotropic Cladding

If the cladding medium is designated by subscript 2, then the displacement vector u can be written in terms of Helmholtz potential functions ϕ_2 (scalar) and A_2 (vector),

$$u_2 = \nabla \phi_2 + \nabla \times A_2 \quad \text{with} \quad \nabla \cdot A_2 = 0 \tag{6}$$

In the absence of body forces and substituting Eq. (6) in Navier's Equation results in the following equations,

$$\nabla \cdot ((\lambda + 2\mu) \nabla^2 \phi_2 - \rho_2 \frac{\partial^2 \phi_2}{\partial t^2}) + \nabla \times (\mu \nabla^2 A_2 - \rho_2 \frac{\partial^2 A_2}{\partial t^2}) = 0 \tag{7}$$

where λ and μ are Lamé constants and ρ is the density. By expanding Eq. (7), four partial differential equations in terms of potential functions are obtained for the cladding. In order to satisfy these partial differential equations, the potential functions must be of the following forms [5]:

$$\begin{aligned}
 \phi_2 &= \sum_{n=0}^{\infty} [E_n J_n(k_{L_2} r) + F_n Y_n(k_{L_2} r)] \cos(n\theta) e^{i(k_z z - \omega t)} \\
 [A_2]_r &= \sum_{n=0}^{\infty} [K_n J_{n+1}(k_{T_2} r) + L_n Y_{n+1}(k_{T_2} r)] \sin(n\theta) e^{i(k_z z - \omega t)} \\
 [A_2]_{\theta} &= \sum_{n=0}^{\infty} [-K_{n+1} J_n(k_{T_2} r) - L_n Y_{n+1}(k_{T_2} r)] \cos(n\theta) e^{i(k_z z - \omega t)} \\
 [A_2]_z &= \sum_{n=0}^{\infty} [M_n J_n(k_{T_2} r) + N_n Y_n(k_{T_2} r)] \sin(n\theta) e^{i(k_z z - \omega t)}
 \end{aligned} \tag{8}$$

where

$$k_{L_2}^2 = \left(\frac{\omega}{c_{L_2}}\right)^2 - k_z^2; \quad k_{T_2}^2 = \left(\frac{\omega}{c_{T_2}}\right)^2 - k_z^2 \tag{9}$$

c_{L_2} and c_{T_2} are the compression and shear wave velocities in the cladding material, respectively. E_n , F_n , K_n , L_n , M_n , N_n are unknown coefficients.

Boundary Conditions

The boundary conditions (continuity of stresses and radial displacement) at the fluid-cladding interface, $r=a$, are:

$$\frac{1}{\rho_w \omega^2} \frac{\partial}{\partial r} (p_i + p_s) = [u_r]_2; [\sigma_{rr}]_2 = -(p_i + p_s); [\sigma_{r\theta}]_2 = 0; [\sigma_{rz}]_2 = 0 \quad (10)$$

where ρ_w is the density of the surrounding fluid. At the core-cladding interface, $r = b$, the corresponding boundary conditions are:

$$\begin{aligned} [\sigma_{r\theta}]_1 &= [\sigma_{r\theta}]_2; [\sigma_{rr}]_1 = [\sigma_{rr}]_2; [\sigma_{rz}]_1 = [\sigma_{rz}]_2 \\ [u_r]_1 &= [u_r]_2; [u_\theta]_1 = [u_\theta]_2; [u_z]_1 = [u_z]_2 \end{aligned} \quad (11)$$

Inserting the potential functions from Eqs. (5) and (8) in Eqs. (10) and (11), results in the following system of ten linear algebraic equations,

$$\begin{aligned} [D_n] \{T_n\} &= \{Q_n\}, \\ \{T_n\} &= [A_n \ B_n \ C_n \ D_n \ E_n \ F_n \ K_n \ L_n \ M_n \ N_n]^T; \\ \{Q_n\} &= [b_1 \ b_2 \ b_3 \ b_4 \ b_5 \ b_6 \ b_7 \ b_8 \ b_9 \ b_{10}]^T; \end{aligned} \quad (12)$$

Eq. (12) can be solved for A_n at any given value of the normalized frequency ka . The individual normal mode for resonances in the far field can be expressed as [11],

$$f_n^{res}(\theta) = \frac{2}{\sqrt{\pi i x}} \varepsilon_n \frac{A_n - A_n^r}{1 + 2 A_n^r} \cos n\theta \quad (13)$$

Moreover, the frequency spectrum and phase diagram can be calculated by

$$f_\infty^{res} = \sum_{n=0}^{\infty} f_n^{res}(\theta) \quad (14)$$

NUMERICAL RESULTS

For studying wave scattering from type I and type II transversely isotropic cylinders, the frequency spectrum and phase diagram for immersed isotropic cylinder, type I and type II transversely isotropic cylinders for various incident angles are calculated. In figure 2 the frequency spectrum and phase diagram of an immersed isotropic aluminium cylinder at various incident angles are shown. The same parameters for cobalt and magnesium cylinders as type I transversely isotropic cylinders are plotted in figures 3 and 4. Figures 5 and 6 show frequency and phase spectra of titanium boride and zinc as type II transversely isotropic materials. As it can be seen in type I materials, figures 3 and 4, as well as isotropic materials, figure 2, at wave incident angles beyond the second critical angle there are no resonances in the frequency and phase spectra. While in type II cylinders, such as titanium boride and zinc as shown in figures 5 and 6, even for wave incidence angles beyond the second and third critical angles, resonance frequencies exist. The critical angles and elastic constants for the above materials are given in table 1.

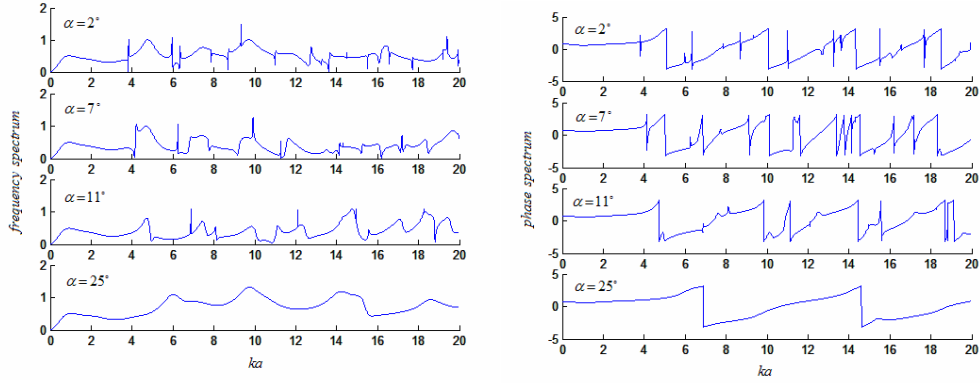


Fig. 2-Frequency spectrum and phase diagram for an immersed aluminium (isotropic) cylinder at various incident angles

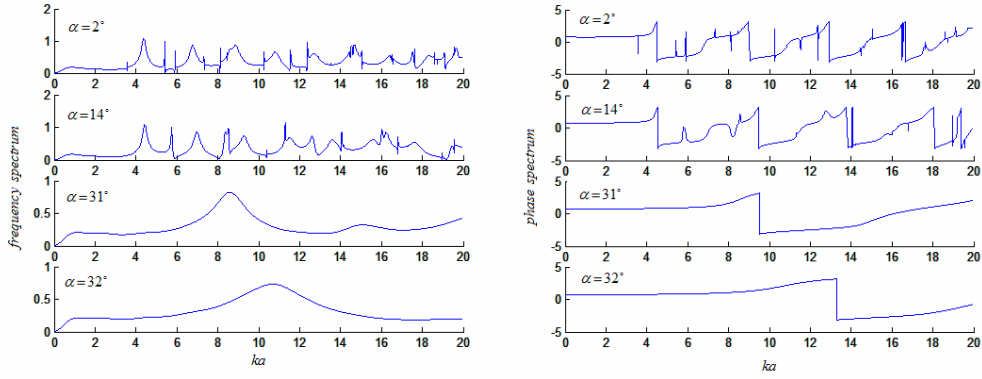


Fig. 3- frequency spectrum and phase diagram for a cobalt (Type I) cylinder at various incident angles

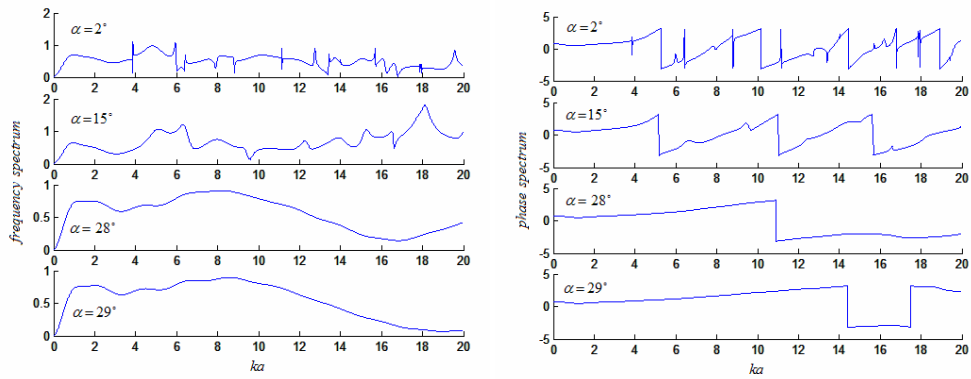


Fig. 4- Frequency spectrum and phase diagram for magnesium (Type I) cylinder at various incident angles

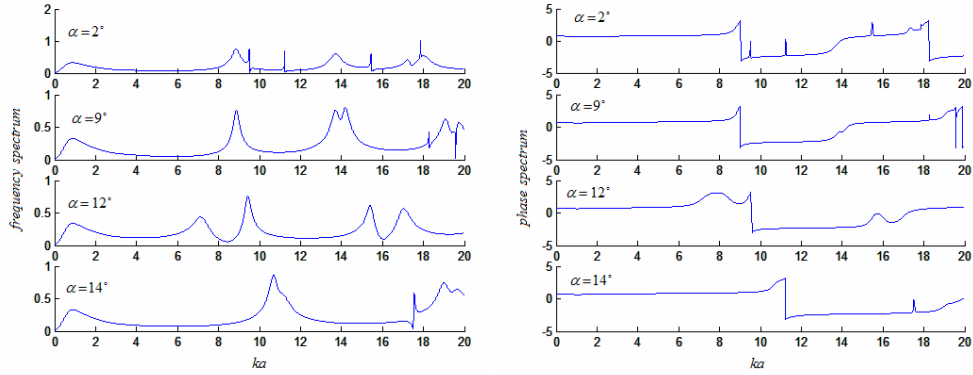


Fig. 5- Frequency spectrum and phase diagram for a titanium boride (Type II) cylinder at various incident angles

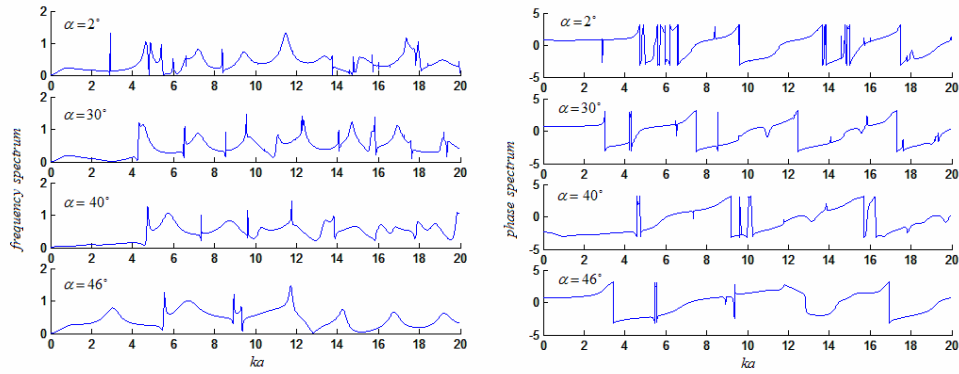


Fig. 6- Frequency spectrum and phase diagram for zinc (Type II) cylinder at various incident angles

Table 1- Material constants and critical angles [6]

Type	Material	Stiffness $\times 10^{11}$ (N/m ²)					Density (kg/m ³)	α_c°
		c_{11}	c_{12}	c_{13}	c_{33}	c_{44}		
I	Magnesium	0.5974	0.2624	0.217	0.617	0.1639	1740	****
I	Cobalt	2.95	1.59	1.11	3.35	0.71	8900	****
II	Cadmium	1.16	0.42	0.41	0.509	0.196	8642	79.38
II	Titanium boride	6.90	4.10	3.20	4.40	2.50	4500	13.86
II	Zinc	1.628	0.362	0.508	0.627	0.385	7140	45.39

CONCLUSION

In this paper, an analytical model is developed for the scattering of acoustic waves from an immersed transversely isotropic rod covered by a cylindrical isotropic cladding. The mathematical formulation is derived for the far-field backscattered amplitude spectrum resulting from oblique insonification of the clad rod. Using the frequency spectrum and phase diagrams, type I and type II transversely isotropic cylinders are studied. It is shown that in type I materials, similar to isotropic materials, at incidence angles larger than the second critical angle, no elastic wave can penetrate into the cylinder and the incident wave is completely reflected. Therefore beyond the second critical angle, no resonance frequencies are observed in frequency spectrum and phase diagram. However, in type II materials, even after the second and third critical angles, resonance frequencies can be observed in the frequency spectrum and phase diagram.

REFERENCES

1. L. Flax and W.G. Neubauer, J. Acoust. Soc. Am. 64, 675 (1978).
2. G.C. Gaunard, Appl. Mech. Rev. 42, 143 (1989).
3. J. Sinai and R. C. Waag, J. Acoust. Soc. Am. 83, 1728 (1988).
4. F. Honarvar and A. N. Sinclair, J. Acoust. Soc. Am. 100, 57 (1996).
5. F. Honarvar and A. N. Sinclair, J. Acoust. Soc. Am. 102, 41 (1997).
6. F. Ahmad and A. Rahman, Int. J. Eng. Sci. 38, 325-335, (2000).
7. F. Honarvar, Y. Fan and A. N. Sinclair, J. Acoust. Soc. Am. 114(1), 45-47 (2003).
8. S. Sodagar, F. Honarvar and A. N. Sinclair, proceeding of ICSV12, Portugal, (2005).
9. J. J. Faran, Jr., J. Acoust. Soc. Am. 23, 405 (1951).
10. P. M. Morse and H. Feshbach, Method of Theoretical Physics (McGraw-Hill, New York), pp. 1764-1767 (1953).
11. H. Rhee and Y. Park, J. Acoust. Soc. Am. 102(6), 3401-3412 (1997).